INTERNATIONAL JOURNAL FOR NUMERICAL METHODS IN FLUIDS, VOL. 8, 405–416 (1988)

NUMERICAL SOLUTIONS OF HIGH-*Re* RECIRCULATING FLOWS IN VORTICITY–VELOCITY FORM

G. GUJ AND F. STELLA

Dipartimento di Meccanica e Aeronautica, Via Eudossiana, 18, 00184 Roma, Italy

SUMMARY

A numerical method for computing high-*Re* laminar steady flows is presented. The incompressible Navier–Stokes equations are expressed in terms of vorticity–velocity variables, discretized in space by finite differences on a staggered grid and advanced in time by a scalar alternating direction implicit (ADI) procedure, which allows a fully vectorized computer code. The accuracy and efficiency of the present formulation are discussed in comparison with the standard ω–ψ and u, v, P forms. Numerical results are presented for two test cases: the driven cavity at *Re* up to 5000 and the backward-facing step at *Re* up to 800.

KEY WORDS Navier–Stokes equations Vorticity–velocity Finite difference

1. INTRODUCTION

The difficulties in obtaining stable and accurate numerical solutions of the incompressible Navier–Stokes equations for laminar flows increase with the Reynolds number and require the use of appropriate mathematical formulation and numerical technique.

Stability can be assured by expressing the convective terms in a convenient form and by adopting appropriate time integration procedures, both measures not requiring large computer storage and CPU time. On the contrary, accuracy is strictly connected with the structure of the flow field, which becomes more and more complex as the Reynolds number increases. In fact, the various recirculating vortices and the high gradients of velocity, located mainly in corner and wall regions, require a high resolution, leading to a very small local mesh size. For this reason in the earlier studies, when computing power had not yet reached the level of mega instruction per second (MIPS) available today, attention was mainly devoted to the issue of stability. For instance, some authors have contributed to the study of stability and thus convergence to steady state of numerical methods, proposing algorithms based on the conservation of integral properties,[1] upwind schemes and numerical viscosity,[2,3] almost Lagrangian grids[4] and adaptive grids.[5]

In the last decade developments in computer hardware technology and in numerical techniques have permitted the treatment of problems with more complex flow structure. Three different techniques may be adopted to obtain the necessary spatial resolution: local mesh refinement,[6] co-ordinate transformation[7] and very fine but uniform mesh.[8–10] The first two approaches allow us to concentrate the computational points only in the critical subregions (boundary or interior layers) of the problem domain, saving computer storage, but the field equations become more complex to account for the non-Cartesian and possibly irregular character of the mesh. The last approach pays for the simplicity of the resulting discretized equations and the accuracy connected with the

0271–2091/88/040405–12$06.00

Received 16 October 1986
Revised 7 May 1987

regularity of the mesh with the need for very large storage and number of operations.

Several mathematical formulations of the Navier–Stokes equations have been developed which may be divided into the following categories, depending on the choice of dependent variables:

(a) primitive variables[7,11,12]
(b) vorticity–streamfunction,[10,13] which in three dimensions extends to the vorticity–vector potential[14,15]
(c) vorticity–velocity.[16–18]

All of these formulations have been used to obtain discretized forms of the Navier–Stokes equations by finite difference or finite element techniques. A variety of numerical results have been presented by many authors for the first two formulations at Reynolds numbers up to 10000; however, only a few studies have been conducted using the last formulation. The earliest contribution was the study of the stability of two-dimensional boundary layers by Fasel[16] which solved the real time-dependent problem by coupling the equation system using an iterative procedure. Dennis *et al.*[17] extended the ω, u, v formulation to three-dimensional steady flows by solving the Navier–Stokes equations in a cubical driven box. Gatski *et al.*[19] applied compact finite difference schemes to the vorticity–velocity form of the two-dimensional unsteady Navier–Stokes equations. Fasel and Booz[20] investigated the axisymmetric supercritical Taylor vortex flow for a wide gap. Farouk and Fusegi[21] studied the natural and forced convection and heat transfer in a two-dimensional annulus. Orlandi[22] solved high-*Re* flows using a block ADI method which coupled field equations and boundary conditions and satisfied the continuity equation without requiring an iterative procedure.

In the present study we describe a numerical technique, based on the vorticity–velocity representation, for calculating steady state solutions of the two-dimensional Navier–Stokes equations. This formulation is simpler than the primitive variable one, because the pressure does not appear explicitly in the field equations so the well-known difficulty connected with the determination of pressure boundary values in incompressible flows[23] is avoided. Furthermore, the use of physical variables ω, u, v makes this formulation more versatile than the ω–ψ one, in particular in the solution of multiconnected problem.[21] It is noteworthy that our numerical tests indicate that the residual trend in the iteration space, the total number of iterations and the steady state solution of the ω, u, v formulation keep very close to those of the ω–ψ approach. Of course the solution of one more Poisson equation requires about 50% more operations in the two-dimensional case, but in the three-dimensional case the number of equations to be solved using the vorticity–velocity representation equals that of the vorticity–vector potential form.[14]

The individual numerical techniques employed in the present study are only partially original and may be summarized in the following steps:

(1) The variables are located on a staggered grid to satisfy better the continuity equation on individual cells.
(2) The equations are discretized by second-order accurate central differences on a uniform Cartesian mesh.
(3) The conservative form is adopted for the vorticity transport equation to verify the conservation of mean vorticity.
(4) The Poisson equations for u and v are parabolized in time so that they are exactly solved at the steady state only.
(5) An alternating direction implicit (ADI) method is used to integrate in time the three equations governing ω, u, v.
(6) The numerical procedures are implemented in a FORTRAN code designed to run efficiently on a vector computer for a typical mesh up to 100×100 points.

The characteristics of the mathematical formulation and the derivation of the basic equations are presented in Section 2. The form of advective term that implies the conservation of integral quantities, in particular of total vorticity, is discussed in Section 3. The characteristics of the discretized equations obtained by the finite difference method, the ADI time integration procedure and the peculiarities of the numerical code are explained in Section 4. The driven cavity problem is considered in Section 5, where the present results are compared with available numerical[8,9,22,24] and experimental[25] findings for Reynolds numbers up to 5000. The flow past a backward-facing step is finally analysed in Section 6, the analysis providing a very convincing proof of the stability of the method even in the presence of a through-flow problem. Experimental measurements[26] and some available numerical results[22,26,27] are used to assess the accuracy of the proposed method. Concluding remarks are reported in Section 7.

2. NAVIER–STOKES EQUATIONS IN TERMS OF VORTICITY–VELOCITY

The Navier–Stokes equations for laminar plane flow of an incompressible fluid may be written in vorticity–transport form as

$$\omega_t + (u\omega)_x + (v\omega)_y = (1/Re)\nabla^2\omega, \tag{1}$$

$$u_x + v_y = 0. \tag{2}$$

Here Re is the Reynolds number

$$Re = u'L/\nu,$$

where ν is the kinematic viscosity and u' and L are a characteristic velocity and length scale respectively. The vorticity ω is defined as

$$\omega = v_x - u_y. \tag{3}$$

If equations (1) and (2) are written in terms of the vorticity ω and streamfunction ψ, the velocity components in the advection term are computed as derivatives of ψ, namely

$$u = \psi_y, \qquad v = -\psi_x, \tag{4}$$

whereas ψ is computed by solving the Poisson equation

$$\nabla^2\psi = -\omega. \tag{5}$$

Taking appropriate derivatives of the vorticity definition (3) and using the continuity condition (2), the following Poisson equations for the velocity components u and v result[16]:

$$\nabla^2 u = -\omega_y, \tag{6}$$

$$\nabla^2 v = \omega_x. \tag{7}$$

Equations (6) and (7) together with (1) represent the complete set of the Navier–Stokes equations in ω, u, v form.

The proposed numerical procedure is based on the discretization of the parabolic equation (1) and the following parabolized version of the velocity equations:

$$Re\,u_t - \nabla^2 u - \omega_y = 0, \tag{8}$$

$$Re\,v_t - \nabla^2 v + \omega_x = 0. \tag{9}$$

The boundary conditions for the driven cavity problem are sketched in Figure 1. In particular, the zero-slip and impermeability conditions are enforced at all solid walls for velocity equations (8) and (9) and boundary conditions for equation (1) are given by the definition of ω, equation (3).

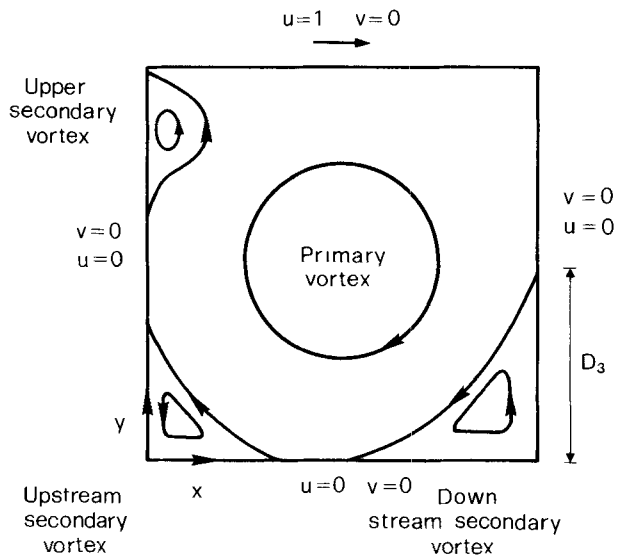

Figure 1. Sketch of a driven cavity, boundary conditions and standing vortices

3. CONSERVATIVE FORM OF THE CONVECTIVE TERM

It is well known that the numerical instabilities and solution inaccuracy at large Re are strongly dependent on the form used for the convective term. To illustrate the importance of the treatment of the convective term and to focus the attention on this aspect only, consider first the vorticity transport equation in divergence form for an inviscid fluid:

$$\omega_t + (u\omega)_x + (v\omega)_y = 0. \tag{10}$$

Since the advection of a scalar quantity (like vorticity) in two-dimensional flow is expressed by a Jacobian, strong integral constraints follow from the nature of the Jacobian itself.[1] In particular, the following quantities have to be conserved in time, in a closed domain with an impermeable boundary: the mean vorticity, the mean kinetic energy and the mean square vorticity (enstrophy). A finite difference scheme should satisfy all these constraints to be fully conservative, leading to Arakawa's spatial discretizations for the advection term. Otherwise the artificially produced quantities may grow, leading to numerical instabilities.

Anyway, for the Navier–Stokes equations the exact conservation of quadratic quantities is not as important as for equation (10), because the square vorticity and the energy possibly generated by the discretized advective term and by the enforcement of the boundary conditions are partially dissipated by the effect of viscosity and do not spoil the stability of the solution. On the otherhand, the mean vorticity must be exactly conserved in the case of Navier–Stokes equations as a consequence of the Stokes theorem, to avoid numerical instabilities. This latter condition is satisfied by either the conservative (divergence) form or the Arakawa scheme,[1] the choice being constrained only to accuracy criteria. Preliminary tests have shown a comparable accuracy of the two forms. The standard conservation form is adopted in the present work because the discrete equations are easily constructed and the boundary conditions on vorticity are straightforward.[10]

4. NUMERICAL MODEL

The governing equations (1), (8) and (9) are discretized by central second-order finite differences and solved on a uniform mesh via the false time-dependent method.[28] The choice of location of

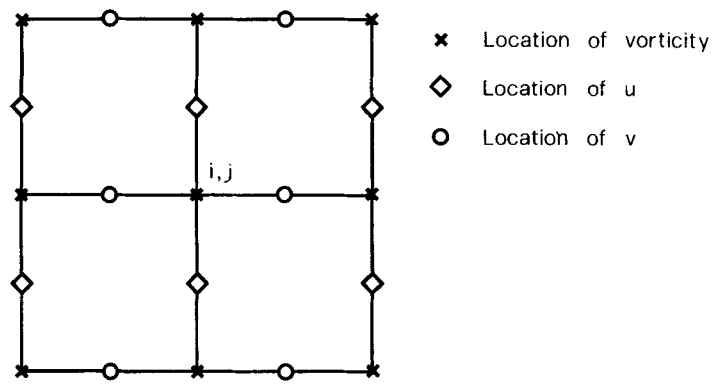

Figure 2. Locations of MAC-like scheme variables

variables in the computational molecule is a crucial point to satisfy the continuity equation if the velocity is taken as one of the unknowns.[29] In the present ω, u, v formulation the mass conservation equation requires the total flux to be zero across cell sides and consequently the velocity components have to be located at the cell midside (Figure 2). In this way the main features of the MAC scheme introduced by Harlow and Welch[29] for the u, v, P representation are adapted to the present approach.

The resulting algebraic problem for large Reynolds numbers is dominated by the non-linear convective terms, and therefore the linearization and the iterative procedure are very important in the solution algorithm. The discretized problem results in a large system of equations of the type

$$\mathbf{A}(\mathbf{x})\mathbf{x} = \mathbf{b}, \tag{11}$$

where $\mathbf{x}$ is the unknown vector and $\mathbf{b}$ is a known vector. The coefficient matrix $\mathbf{A}$ is a large 3×3 block matrix with a banded and sparse structure. The direct solution of equation system (11) is not possible due to the non-linearity of the problem, so that an iterative procedure is required. The splitting of the time step overcomes the problem of storing and inverting matrix $\mathbf{A}$, because in each half time step $\mathbf{A}$ is reduced to a sequence of 3×3 block tridiagonal problems which can be solved by a block tridiagonal procedure.

We propose the use of the simpler ADI procedure of scalar type for each of the three equations separately to give a fully and easily vectorizable algorithm.

The line iteration is organized in such a way that the equations are coupled at the same half time step for velocity equations and at the previous half time step for vorticity equations, as explained in the following. In particular, these minor differences appear in comparison with the block ADI method:

(i) The non-linear convective term

$$(u\omega)_x + (v\omega)_y \tag{12}$$

should be computed at the new half time step $n + 1/2$:

$$(u^{n+1/2}\omega^{n+1/2})_x + (v^n\omega^n)_y. \tag{13}$$

In the block ADI method this term may be discretized in time as[22]

$$(u^{n+1/2}\omega^n)_x + (u^n\omega^{n+1/2})_x - (u^n\omega^n)_x + (v^n\omega^n)_y. \tag{14}$$

In the proposed scalar ADI method the term becomes

$$(u^n\omega^{n+1/2})_x + (v^n\omega^n)_y. \tag{15}$$

At the second half time step $n+1$ the term (12) is treated analogously.

(ii) Boundary conditions on the vorticity ω cannot be enforced at the same time step n as is possible with block ADI algorithm,

$$\omega^n = v_x^n - u_y^n, \tag{16}$$

but at the previous half time step $n-1/2$,

$$\omega^n = v_x^{n-1/2} - u_y^{n-1/2}. \tag{17}$$

All the other terms are treated in the same way by the two methods. In a preliminary work we have compared the efficiency and stability of block ADI and scalar ADI methods for high-Re flows, finding quite similar stability characteristics but a computation time about four times greater for the block ADI method. In fact both methods require a large number of iterations to find the steady state solution, owing to the non-linear convective term described in (i) and the splitting in time of the vorticity–transport equation (1) and the parabolized velocity equations (8) and (9).

The discretized form of the time derivative of the vorticity in equation (1) and the relaxation-like time derivative in equations (8) and (9) are exactly the same, so that the three derivatives vanish analogously when the steady state solution is reached and a Δt of the same order of magnitude can be adopted for the three equations.

To verify the stability characteristics of the proposed method in comparison with the standard ω–ψ formulation, equation (5) as also parabolized in time, as previously described, to obtain the governing equations proposed by Benjamin and Denny.[10]

To highlight the difference between the two formulations, the driven cavity problem (Figure 1) is solved for Re up to 5000 using the same time step and discretization grid (40 × 40). Very close residual trends in time and the number of iterations are obtained for the two formulations. Moreover, the steady solutions coincide, as shown by the extreme values of velocity reported in Table I for $Re = 400$ and 5000. The extremes in velocity of the solution obtained by the artificial compressibility method[11] using a staggered mesh[30] are also shown in Table I. The comparison shows that the difference is less than 0·2%.

Because of the large number of grid points and iterations involved, particular attention is devoted to the vectorization of the numerical code so that a CRAY-1 computer may be usefully utilized. The scalar ADI approach is particularly suited to this purpose, since in the splitting operation the linear systems of equations, derived by the discretization of each line, are uncoupled. Therefore they may be solved simultaneously, leading to a fully vectorized code.

The efficiency of the proposed code in comparison with one that is not vectorized is clearly

Table I. Extremes in velocity for the driven cavity problem

	$Re = 400$			$Re = 5000$	
	ω, u, v	ω–ψ	u, v, P	ω, u, v	ω–ψ
	40 × 40	40 × 40	40 × 40	40 × 40	40 × 40
$u_{\min}$	−0·3180	−0·3180	−0·3178	−0·3124	−0·3124
$v_{\max}$	0·3024	0·3024	0·3020	0·3022	0·3022
$v_{\min}$	−0·6033	−0·6033	−0·6032	−0·5352	−0·5352

Table II. CPU time in seconds

	11 × 11	21 × 21	41 × 41
CRAY-1 vectorized	0·13	1·0	6·5
CRAY-1 scalar	0·37	4·5	43·4
UNIVAC 1100	2·00	55·0	480·0

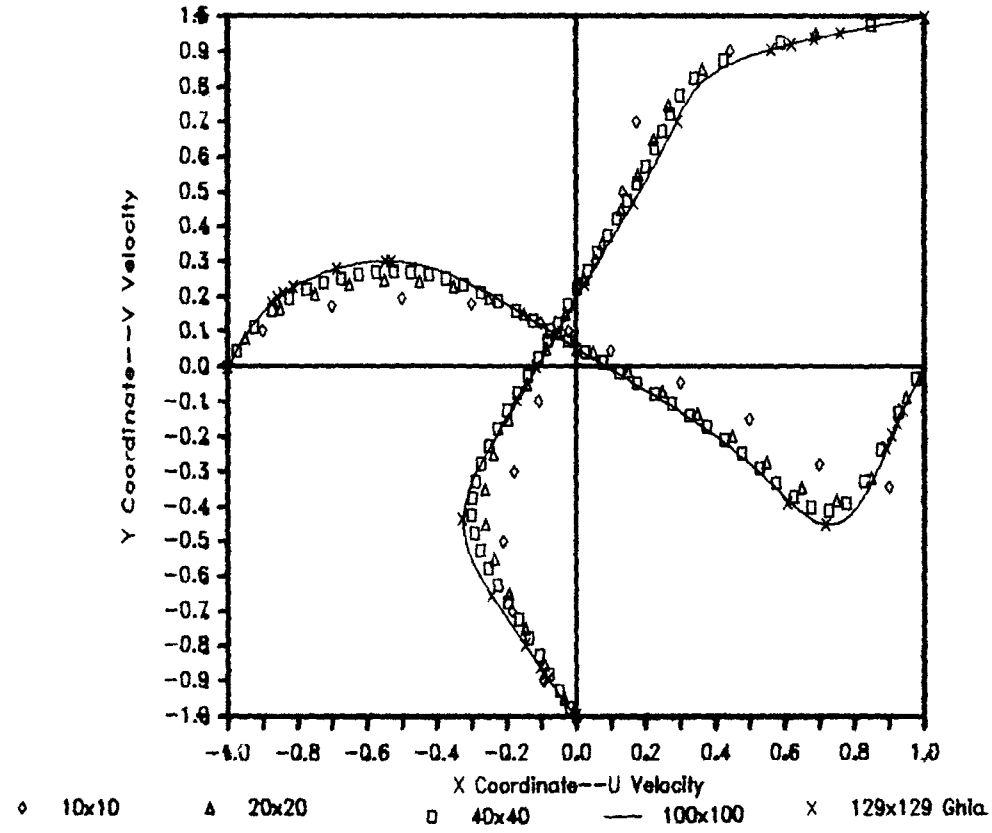

Figure 3. Mesh dependence at $Re = 400$

demonstrated by the computer time needed, on the CRAY-1, to solve the driven cavity test case for different numbers of grid points, as shown in Table II.

5. DRIVEN CAVITY TEST CASE

A lid driven cavity problem has been studied first, a large number of numerical bench-mark solutions and a few experimental results being available. The geometry of the domain, the boundary conditions and the nomenclature of several standing vortices are shown in Figure 1.

Our attention is first devoted to the evaluation of the grid dependence. The numerical prediction of Ghia *et al.*[8] is taken as the reference solution at $Re = 400$.

In Figure 3 both u and v velocity components at the middle are plotted for an increasing number of grid points up to 100 × 100 and compared with Ghia *et al.*'s results obtained with

a 129 × 129 grid via a multigrid technique. Very good agreement is found for both maximum velocity position and value. At $Re = 5000$ good agreement is found only for the position; the maximum velocity predicted for a 100 × 100 grid is about 8·5% less than that of Ghia *et al.* obtained with 257 × 257 grid points as shown in Figure 4. This is explained by poor resolution of the boundary layer for Re larger than 1000.

To give more quantitative information on the extremes in velocity, the present values are compared with those of Ghia *et al.*[8] and Gresho *et al.*[31] for $Re = 1000$, 3200 and 5000 in Table III.

The size of the downstream secondary eddy as a function of Re is taken as a characteristic macroscopic quantity because it seems to show the largest discrepancies between the numerical predictions. In Figure 5 the predicted and measured dimensionless sizes D_3/D of the downstream secondary eddy are plotted as reported by Koseff and Street,[25] together with the present numerical results.

All the numerical studies agree well each other but predict a separation region larger than that observed experimentally. In particular, the present results, like most of the others, show a linear trend on a semilog scale if a constant uniform grid is used, independent of the Reynolds number. Consider, for example, the Ghia *et al.* predictions: they are located on two parallel straight lines with a vertical translation at Re between 3200 and 5000 for which the mesh size is changed; in fact

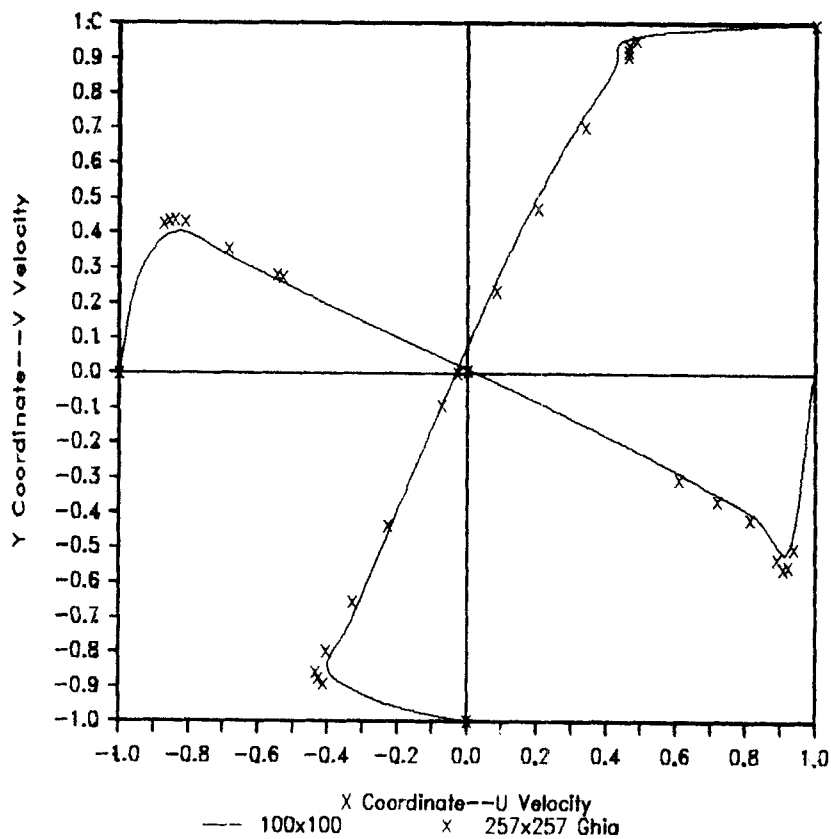

Figure 4. Velocity profiles at $Re = 5000$

Table III

Re	Author	$u_{min}(x=0{\cdot}5)$ u_{min}	y	$v_{min}(y=0{\cdot}5)$ v_{min}	x	$v_{max}(y=0{\cdot}5)$ v_{max}	x
1000	Gresho *et al.*[31]	−0·375	0·160	−0·516	0·906	0·362	0·160
	Ghia *et al.*[8]	−0·388	0·172	−0·516	0·906	0·371	0·156
	Present results	−0·378	0·176	−0·514	0·905	0·368	0·155
3200	Gresho *et al.*[31]	−0·420	0·084	−0·560	0·945	0·415	0·094
	Ghia *et al.*[8]	−0·419	0·102	−0·541	0·945	0·428	0·094
	Present results	−0·404	0·095	−0·528	0·945	0·403	0·105
5000	Gresho *et al.*[31]	−0·426	0·074	−0·563	0·906	0·419	0·074
	Ghia *et al.*[8]	−0·436	0·070	−0·554	0·953	0·436	0·078
	Present results	−0·399	0·075	−0·516	0·955	0·404	0·085

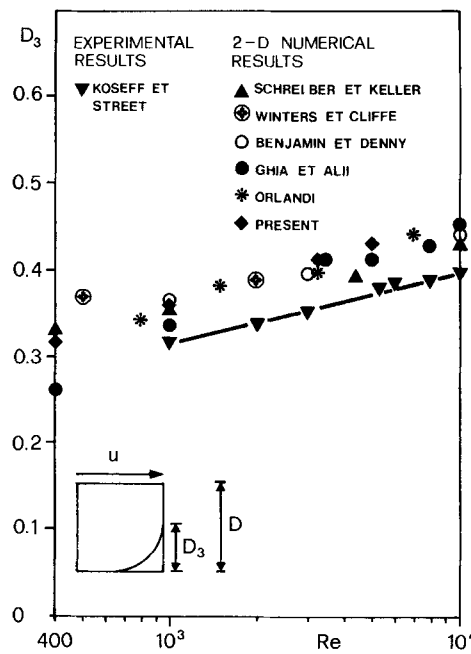

Figure 5. Driven cavity: size of downstream secondary vortex $D_3(=D_3/D)$

they are computed with 129 × 129 and 257 × 257 grid points respectively. The smallest value of the experimental results is due[25] mainly to Taylor–Gortler-like vortices connected with the three-dimensionality of the flow field. Reynolds numbers greater than 5000 are not considered, because a grid size finer than 100 × 100 would be required in order to resolve the fine details of the flow. Koseff *et al.*[25] also observed the onset of turbulence at $Re \simeq 6000$.

6. BACKWARD-FACING STEP

The backward-facing step is considered to verify the stability and accuracy of the proposed method when analysing an inflow–outflow problem. A sketch of the integration domain, boundary

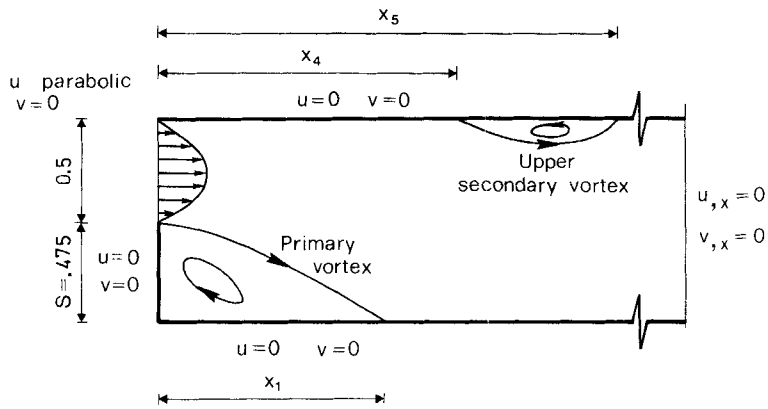

Figure 6. Sketch of backward-facing step, boundary conditions and standing vortices

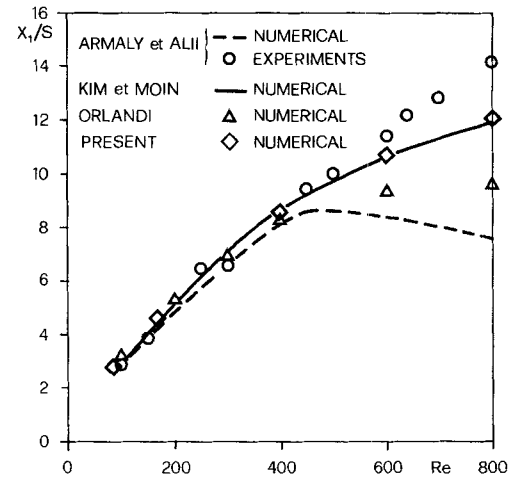

Figure 7. Backward-facing step: non-dimensional size of primary vortex (x_1/S)

conditions and nomenclature of the eddies is shown in Figure 6. The Reynolds number is defined[26] using the mean velocity in the inlet section and twice its height as reference velocity and length respectively. The solutions at $Re \simeq 800$ are obtained with 40×101 grid points for an expansion ratio of 1·95, the same as in the experiments of Armaly *et al.*[26]

The length of the computational domain is chosen equal to about three times the experimentally measured length of the primary vortex.[26] A parabolic u velocity profile is imposed at the inflow boundary together with a zero vertical velocity v. Non-slip and impermeability conditions are enforced on solid walls and Neumann conditions for both u and v are imposed at the outflow boundary. It is noteworthy that almost identical results are obtained if fully developed Dirichlet conditions (u parabolic, v zero) are used also at the outflow, as already found by Kim and Moin[27] using u, v, P variables.

Figure 7 shows the reattachment length of the primary vortex as a function of Reynolds number.

The present predictions are compared with the experimental measurements of Armaly *et al.*[26] and with the numerical results of Armaly *et al.*,[26] Kim and Moin[27] and Orlandi.[22] Good agreement is found withexperiment (maximum difference 15% at $Re = 800$) and almost perfect

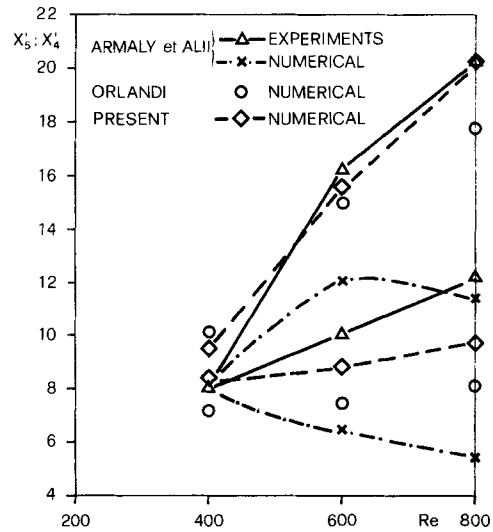

Figure 8. Backward-facing step: non-dimensional size of X_4, X_5

correspondence is achieved with Kim and Moin[27] who use 100×100 mesh points. The reattachment lengths found by Orlandi[22] are in lesser agreement with the experiments, owing to the use of a coarser non-uniform mesh (20×50). The Armaly *et al.*[26] numerical predictions are, as observed also by Kim and Moin,[27] inaccurate at $Re = 400$, owing to the use of an upwind scheme for the treatment of the convective term. The predicted locations of the detachment and reattachement lengths of the upper secondary eddy as a function of Re are shown in Figure 8 in comparison with available experimental[26] and numerical[22,26] results. The trend of both position and dimension with Re is in very good agreement with the experimental results.[26]

7. CONCLUSIONS

The test cases considered, in the steady state flow at high Reynolds numbers, have highlighted several attractive features of the proposed numerical method based on the Navier–Stokes equations in term of the physical variables ω, u, v:

(1) The results are as accurate as those obtained by the standard ω–ψ or u, v, P formulation if an equivalent second-order accurate spatial discretization is adopted for all three forms.
(2) The solution algorithm, based on a false time-dependent procedure and on the parabolized form of the Poisson velocity equations, is particularly stable and efficient in that an ADI method is adopted for each equation.
(3) The conservative formulation of convective terms and the staggered location of velocity components have demonstrated an exact mass and mean vorticity conservation, the order of magnitude of the residual of the continuity equation and Stokes theorem equalling the order of magnitude of the residual of the vorticity equations.

ACKNOWLEDGEMENTS

The authors are pleased to acknowledge the suggestions and interest of Professors P. Orlandi and L. Quartapelle.

REFERENCES

1. A. Arakawa, 'Computational design for long term numerical integration of the equations of fluid motion: two-dimensional incompressible flow', *J. Comput. Phys.*, **1,** 119 (1966).
2. C. W. Hirt, 'Heuristic stability theory for finite-difference equations', *J. Comput. Phys.*, **2,** 339 (1968).
3. J. E. Fromm, 'Practical investigation of convective difference approximations of reduced dispersion', *Phys. Fluids*, **3,** Suppl. II (1969).
4. C. W. Hirt, A. A. Amsden and J. L. Cook, 'An arbitrary Lagrangian–Eulerian computing method for all flow speeds', *J. Comput. Phys.*, **14,** 227 (1974).
5. R. Piva, A. Di Carlo, B. Favini and G. Guj, 'Adaptive curvilinear grid for large Reynolds number viscous flows', *Lecture Notes in Physics*, **170,** Springer-Verlag, 1982, p. 414.
6. J. Ruge and K. Stuben, 'Efficient solution of finite difference and finite element equations', in D. L. Paddon (ed.), *Proc. Multigrid Methods for Integral and Differential Equations*, 1985, p. 169.
7. R. Piva, A. Di Carlo and G. Guj, 'Finite element MAC scheme in general curvilinear coordinates', *Comput. Fluids*, **8,** 225 (1986).
8. U. Ghia, K. N. Ghia and C. T. Shin, 'High-*Re* solutions for incompressible flow using the Navier–Stokes equations and a multigrid method', *J. Comput. Phys.*, **48,** 387 (1982).
9. R. Schreiber and H. B. Keller, 'Driven cavity flows by efficient numerical techniques', *J. Comput. Phys.*, **49,** 310 (1983).
10. A. S. Benjamin and V. E. Denny, 'On the convergence of numerical solutions for 2-D flows in a cavity at large *Re*', *J. Comput. Phys.*, **33,** 340 (1979).
11. A. J. Chorin, 'A numerical method for solving incompressible viscous flow problems', *J. Comput. Phys.*, **2,** 12 (1967).
12. P. M. Gresho, S. T. Chan, R. L. Lee and C. D. Upson, 'A modified finite element method for solving the time-dependent, incompressible Navier–Stokes equations. Part 1: Theory', *Int. j. numer. methods fluids*, **4,** 557 (1984).
13. J. E. Fromm and F. H. Harlow, 'Numerical solution of the problem of vortex street development', *Phys. Fluids*, **6**(7), 975 (1963).
14. G. D. Mallison and C. De Vahl Davis, 'Three dimensional natural convection in a box: a numerical study', *J. Fluid Mech.*, **83,** 1 (1977).
15. S. M. Richardson and A. R. Cornish, 'Solution of three dimensional incompressible flow problems', *J. Fluid Mech.*, **82,** 309 (1967).
16. H. Fasel, 'Investigation of the stability of boundary layers by a finite-difference model of the Navier–Stokes equations', *J. Fluid Mech.*, **78**(2), 355 (1976).
17. S. C. R. Dennis, D. B. Ingham and R. N. Cook, 'Finite-difference methods for calculating steady incompressible flows in three-dimensions', *J. Comput. Phys.*, **33,** 325 (1979).
18. R. K. Agarwal, 'A third-order-accurate upwind scheme for Navier–Stokes solutions in three dimensions', *Proc. ASME*, Washington, DC, November 1981.
19. T. B. Gatski, C. E. Grosh and M. E. Rose, 'A numerical study of the two-dimensional Navier–Stokes equations in vorticity–velocity variables', *J. Comput. Phys.*, **48,** 1 (1982).
20. H. Fasel and O. Booz, 'Numerical investigation of supercritical Taylor-vortex flow for a wide gap', *J. Fluid Mech.*, **138,** 21 (1984).
21. B. Farouk and T. Fusegi, 'A coupled solution of the vorticity–velocity formulation of the incompressible Navier–Stokes equations', *Int. j. numer. methods fluids*, **5,** 1017 (1985).
22. P. Orlandi, 'Vorticity–velocity formulation for high Reynolds number flows', *Comput. Fluids*, **15**(2), 137 (1987).
23. L. Quartapelle and M. Napolitano, 'Integral condition for the pressure in the computation of incompressible viscous flows', *J. Comput. Phys.*, **62,** 340 (1986).
24. K. Winters and K. Cliffe, 'A finite element study of driven laminar flow in a square cavity', *UKAERE Harwell Report R9444*, 1979.
25. J. R. Koseff and R. L. Street, 'Visualization studies of a shear driven three-dimensional recirculating flow', *Trans. ASME*, **106,** 22 (1984).
26. B. F. Armaly, F. Durst, J. C. F. Pereira and B. Schnung, 'Experimental and theoretical investigation of backward-facing step flow', *J. Fluid Mech.*, **127,** 473 (1983).
27. J. Kim and P. Moin, 'Application of a fractional step method to incompressible Navier–Stokes equations', *J. Comput. Phys.*, **59,** 308 (1985).
28. P. Roache, *Computational Fluid Dynamics*, Hermosa Publ., 1972.
29. F. Harlow and J. E. Welch, 'Numerical calculation of time dependent viscous incompressible flow of fluid with free surface...', *Phys. Fluids*, **8,** 2182 (1965).
30. C. W. Hirt and J. L. Cook, 'Calculating three-dimensional flows around structures and over rough terrain', *J. Comput. Phys.*, **10,** 324 (1972).
31. P. M. Gresho, S. T. Chan, R. L. Lee and C. D. Upson, 'A modified finite element method for solving the time-dependent incompressible Navier–Stokes equations. Part 2: Applications', *Int. j. numer. methods fluids*, **4,** 619 (1984).